Synthesis of crystallized mesoporous transition metal oxides by silicone treatment of the oxide precursor

Nao Shirokura,[a] Kiyotaka Nakajima,[a] Akira Nakabayashi,[b] Daling Lu,[c] Michikazu Hara,[a] Kazunari Domen,[d] Takashi Tatsumi[a] and Junko N. Kondo*[a]

Received (in Cambridge, UK) 1st March 2006, Accepted 3rd April 2006
First published as an Advance Article on the web 21st April 2006
DOI: 10.1039/b603115c

Ordered mesoporous transition metal oxides were successfully crystallized after strengthening the amorphous framework by a silica layer, which efficiently protected the original mesoporous structure against crystallization and resulting mass transfer.

Although much less research has been conducted on the synthesis of mesoporous transition metal oxides[1–4] compared to silica materials,[5–8] there is sustained interest in this field and the volume of literature continues to increase through the accumulated efforts of many researchers. Most research in this area has involved the development of new and unique properties of transition metal oxides based on mesoporous structures, including magnetic,[9] electronic[10] and catalytic[4,11–13] properties that cannot be realized using silica materials. However, the performance of transition metal oxides as functional materials is limited in the amorphous state, where the specific electronic orbitals and lattice defects frequently responsible for catalysis are absent. Thus, crystallization of mesoporous transition metal oxides is required if they are to be utilized in wide range of applications. At the initiation of crystallization, which occurs at temperatures below those required for complete crystallization, mesoporous Ti, Zr and Nb oxides develop nano-crystalline patches in the amorphous walls.[1,2] Further crystallization by heating at higher temperatures gives rise to drastic mass transfer due to complete phase transition from amorphous to crystalline with large crystal domains, typically resulting in a collapse of the mesoporous structure and affording a material with lower surface area and porosity.[14,15] Therefore, highly crystallized mesoporous transition metal oxides with the original mesoporous structure cannot be obtained spontaneously.

To overcome this problem, strengthening the pore walls prior to crystallization is regarded to be indispensable.[16] Our group has previously attempted to achieve this type of wall strengthening by filling the pores of hexagonal mesoporous Nb–Ta mixed oxide with carbon material (similar to CMK[17] materials) and calcining the samples in an inert atmosphere to induce crystallization.[18] The carbon could be subsequently removed by calcination in air to afford crystallized Nb–Ta mixed oxide with the original hexagonal mesopore structure. However, while this approach was successful in some cases, it is not generally applicable due to the difficulty in achieving complete carbon filling.

As an alternative approach, the internal and external surfaces of mesoporous transition metal oxides were treated in this study with a silicone compound, bis(trimethylsiloxy)methylsilane (BTMS; $(CH_3)_3Si–O–SiH(CH_3)–O–Si(CH_3)_3$), to fortify the pore walls against mass transfer upon crystallization. In silicone treatment, the surface hydroxyl groups of the mesoporous transition metal oxides reacted with the Si–H bonds to form M–O–Si (M = metal cation) bonds. The samples were then calcined in air to induce crystallization, during which the silicone compounds were converted to silica through the combustion of methyl groups. The crystallized materials were finally treated with alkaline solution to remove the silica layer, affording a crystallized mesoporous transition metal oxide with the original hexagonal mesoporous structure. Tantalum oxide[19] was one of the most successful of the mesoporous transition metal oxides treated by this process.

The amorphous precursor, a hexagonal mesoporous Ta oxide, was prepared by a previously reported procedure. The amorphous precursor of the hexagonal Ta oxide (0.7–1.4 g) was pretreated at 70 °C, after which five portions of BTMS was added dropwise to the solution followed by stirring for 5 h at the same temperature. The silicone-treated mesoporous materials were then obtained upon removal of unreacted BTMS by heating at 70 °C for 1 h under evacuation. Crystallization was performed by calcination in air at temperatures determined by TG-DTA analysis. The silicate layer was subsequently removed by treatment with alkaline solution (pH 14) at 100 °C for 10–20 min several times until no change was observed in the N_2 sorption results. The final products were collected by filtration and drying under ambient conditions.

The thermogravimetry/differential thermal analysis (TG-DTA) results for the original amorphous mesoporous Ta oxide before and after silicone treatment are first compared in Fig. 1. The DTA peak for the non-treated mesoporous Ta oxide occurs at 770 °C without weight loss, assignable to the crystallization temperature of the amorphous Ta oxide.[20] For the silicone-treated sample, an exothermal peak appears at 500–550 °C associated with considerable weight loss, attributable to the combustion of methyl groups in BTMS. Thus, at temperatures higher than 550 °C, the stabilized BTMS is converted to silica on the amorphous walls of the mesoporous Ta oxide. An additional peak observed in Fig. 1B without an associated weight loss at 845 °C is due to crystallization of the silicone-treated mesoporous Ta oxide. It should be noted that the silicone treatment increases the crystallization temperature,

[a]*Chemical Resources Laboratory, Tokyo Institute of Technology, 4259 Nagatsuta, Midori-ku, Yokohama, 226-8503, Japan. E-mail: jnomura@res.titech.ac.jp; Fax: +81-45-924-5282; Tel: +81-45-924-5265*
[b]*Performance Materials R&D Center, Asahi Kasei Chemicals Co., Ltd., Kawasaki-ku, Kawasaki, 210-0863, Japan*
[c]*Research Office of Solution-Oriented Research for Science and Technology (SORST), Japan Science and Technology (JST), Nihonbashi 3-4-15, Yaesudori Bldg. 9F, Chuo-ku, Tokyo, 103-0027, Japan*
[d]*Department of Chemical System Engineering, The University of Tokyo, 7-3-1, Hongo, Bunkyo-ku, Tokyo, 113-8656, Japan*

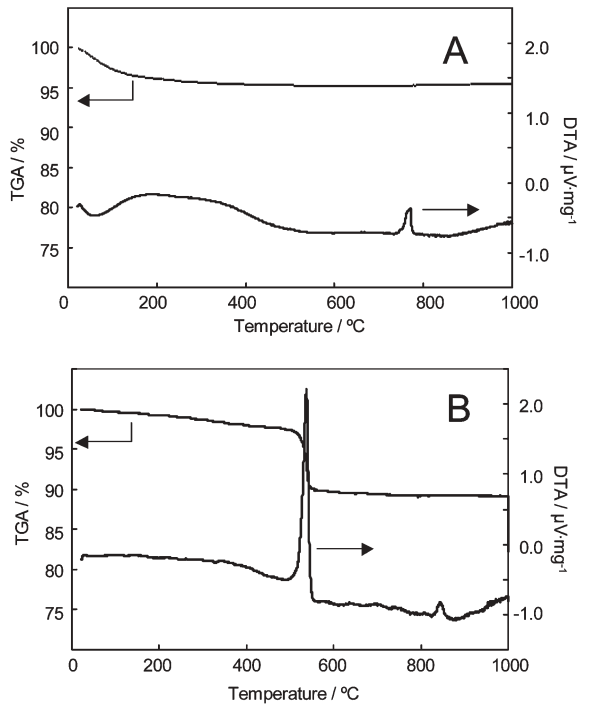

Fig. 1 TG-DTA data for (A) mesoporous Ta_2O_5 and (B) silicone-treated mesoporous Ta oxide.

most probably due to the inhibition of mass transfer of amorphous Ta oxide upon crystallization. This remarkable increase in crystallization temperature was also observed for Nb, Nb–Ta and Mg–Ta oxides. In this study, the crystallization of amorphous mesoporous Ta oxide was performed at 845 °C for 1 h.

Small- and wide-angle X-ray diffraction (XRD) patterns of the mesoporous Ta oxide at various steps in the crystallization procedure are presented in Fig. 2. A diffraction peak observed at 1.42° for the amorphous mesoporous Ta oxide (Fig. 2A(b)) is due to the mesoporous structure, and its amorphous structure is confirmed in Fig. 2B(b). Crystallization of the amorphous mesoporous Ta oxide without modification causes the diffraction peak in Fig. 2A to disappear (Fig. 2A(a)) due to pore collapse, as confirmed in Fig. 2B(a). After silicone treatment, no significant

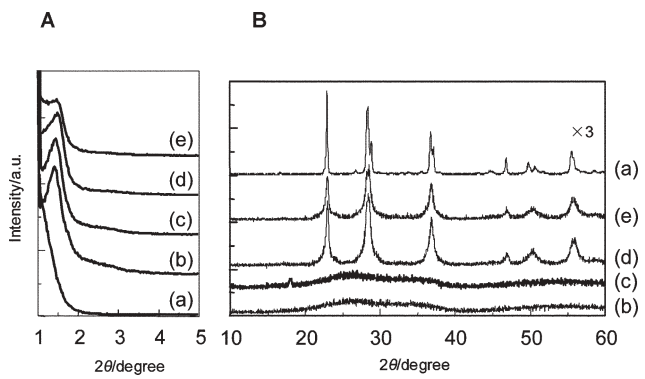

Fig. 2 (A) Small- and (B) wide-angle XRD patterns for (a) the crystallized sample without silicone treatment, (b) the amorphous precursor, (c) the silicone-treated precursor, (d) the silicone-treated sample after crystallization, and (e) the silicone-treated sample after crystallization and alkaline treatment.

change from the amorphous precursor is observed in either diffraction pattern (Fig. 2A(c) and B(c)), although there is a change in apparent pore size, as mentioned below. Intense diffraction peaks supporting crystallization are observable in Fig. 2B(d) after calcination of the silicone-treated sample at 845 °C for 1 h, analogous to the as-crystallized sample in Fig. 2B(a). In the same crystallized sample, a diffraction peak is still observable at 1.50° (Fig. 2A(d)), indicating the preservation of the original mesostructure in the silicone-treated and crystallized sample. This crystallized mesostructure is also retained upon removal of the silica by alkaline treatment (Fig. 2A(e) and B(e)). Therefore, the original mesoporous structure is expected to be present in the sample crystallized in the present method.

The pore structure was examined based on the N_2 adsorption–desorption isotherms of the samples shown in Fig. 2. The isotherms are shown in Fig. 3, and the physico-chemical properties obtained from both XRD and N_2 sorption analyses are summarized in Table 1. The original mesoporous amorphous Ta oxide exhibits the type-IV isotherm pattern typical of mesoporous materials (Fig. 3(b)), with a BET surface area of 152 $m^2\ g^{-1}$ and pore size of 3.6 nm. The isotherm of the original amorphous mesoporous Ta oxide changed drastically upon crystallization (Fig. 3(a)) and the BET surface area decreased to 33 $m^2\ g^{-1}$, indicating that the original mesoporous structure had been lost. The BET surface area and pore volume are slightly lower in the silicone-treated amorphous sample due to the presence of silica in the mesopores, as confirmed by the decrease in pore size from 3.6 to 2.5 nm. However, the BET surface area, pore volume and pore size remain almost unchanged upon crystallization (Table 1), and the pore size increases to 3.1 nm upon removal of the silica by alkaline treatment. This slight decrease in pore size from 3.6 nm in the initial amorphous precursor (Table 1(b)) to 3.1 nm in the final product (Table 1(e)) is most probably due to shrinkage of the walls upon crystallization, and is consistent with the decrease in the repeat distance of samples after crystallization (Table 1). Thus, the pore size is reduced by 1.1 nm by BTMS treatment, recovered by 0.5 nm by silica removal, and reduced by 0.5 nm by wall shrinkage.

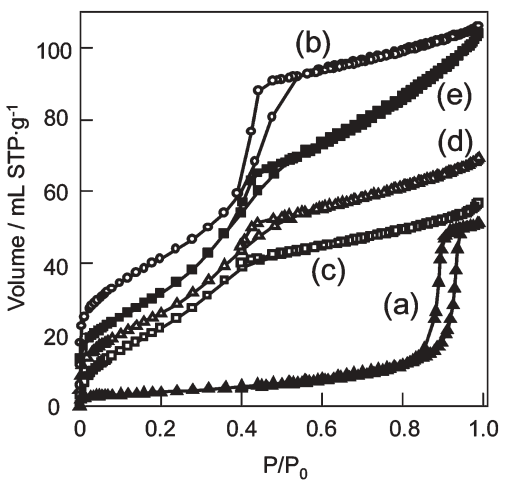

Fig. 3 N_2 adsorption–desorption isotherms for (a) the crystallized sample without silicone treatment, (b) the amorphous precursor, (c) the silicone-treated precursor, (d) the silicone-treated sample after crystallization, and (e) the silicone-treated sample after crystallization and alkaline treatment.

Table 1 Physicochemical properties of mesoporous tantalum oxide

	BET surface area/m^2 g^{-1}	Pore volume/mL g^{-1}	Pore size/nm	Repeat distance/nm
(a) As-crystallized Ta oxide	33	0.15	—	—
(b) Amorphous precursor	152	0.20	3.6	6.2
(c) Silicone-treated mesoporous Ta oxide	102	0.10	2.5	6.5
(d) (c) after crystallization	109	0.13	2.6	6.5
(e) (d) after alkaline treatment	131	0.20	3.1	6.5

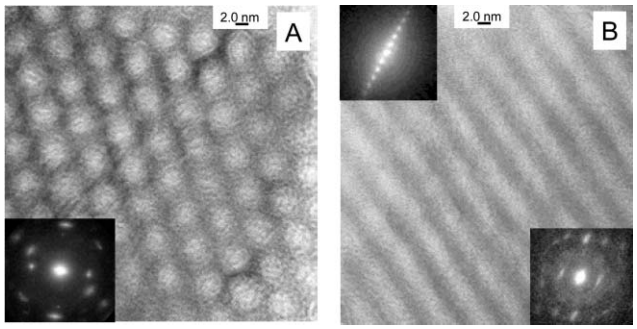

Fig. 4 TEM images and ED patters (inset) of silicone treated mesoporous Ta_2O_5 after (A) crystallization and (B) alkaline treatment.

This indicates that the pore size of the crystallized silicone-treated sample is reduced by lattice shrinkage and increased by methyl combustion, resulting in a negligible overall change in pore size. The silica layer formed by the combustion of silane within the mesopore was confirmed to be effectively removed by ICP analysis.

The presence of mesopores with crystallized walls was confirmed by direct transmission electron microscopy (TEM) observation of pores and lattice fringes. Fig. 4A shows a typical TEM image of the silicone-treated, crystallized mesoporous Ta oxide and electron diffraction (ED) pattern (inset). Highly ordered mesopores can be clearly observed, with lattice fringes appearing simultaneously in several directions. The spot pattern in the ED pattern further confirms that crystallization has been achieved. It should be noted that the central spot in the ED pattern forms a hexagonal pattern, indicating the co-existence of two different ordered structures at the atomic and nano-levels. The well-ordered and crystallized mesoporous structure is preserved after silica removal as shown in Fig. 4B. The ED patterns in Fig. 4B were measured at two different focal distances to confirm both the mesoporous ordering (upper inset) and crystallization (lower inset). The nano-scale periodicity is also indicated by the diffraction spots (see the central spot in the lower inset), further confirming that the material consists of single-crystal domains. Although the particles are polycrystalline, no inter-particle voids exist between crystal domains, and the original ordered mesopores remain present. Comparing with the carbon back-filling method,[18] this silicone treatment method more efficiently retains the original ordered mesoporous structure upon crystallization, and as such appears to be an excellent and widely applicable strategy for the synthesis of crystalline mesoporous transition metal oxides.

Notes and references

1 P. Yang, D. Zhao, D. I. Margolose, B. F. Chmelka and G. D. Stucky, *Nature*, 1998, **396**, 152.
2 P. Yang, D. Zhao, D. I. Margolose, B. F. Chmelka and G. D. Stucky, *Chem. Mater.*, 1999, **11**, 2813.
3 F. Schüth, *Chem. Mater.*, 2001, **13**, 3184.
4 X. He and D. Antonelli, *Angew. Chem., Int. Ed.*, 2002, **41**, 214.
5 C. T. Kresge, M. E. Leonowicz, W. J. Roth, J. C. Vartuli and J. S. Beck, *Nature*, 1992, **359**, 710.
6 D. Zhao, J. Feng, Q. Huo, N. Melosh, G. H. Fredrickson, B. F. Chmelka and G. D. Stucky, *Science*, 1998, **279**, 548.
7 D. Zhao, Q. Huo, J. Feng, B. F. Chmelka and G. D. Stucky, *J. Am. Chem. Soc.*, 1998, **120**, 6024.
8 S. Che, A. E. Garcia-Bennett, T. Yokoi, K. Sakamoto, H. Kunieda, O. Terasaki and T. Tatsumi, *Nat. Mater.*, 2003, **2**, 801.
9 J. W. Long, M. S. Logan, C. P. Rhodes, E. E. Carpenter, R. M. Stroud and D. R. Rolison, *J. Am. Chem. Soc.*, 2004, **126**, 16879.
10 T. T. Emons, J. Li and L. F. Nazar, *J. Am. Chem. Soc.*, 2002, **124**, 8516.
11 Y. Takahara, J. N. Kondo, T. Takata, D. Lu and K. Domen, *Chem. Mater.*, 2001, **13**, 1194.
12 M. Hiyoshi, B. Lee, D. Lu, M. Hara, J. N. Kondo and K. Domen, *Catal. Lett.*, 2004, **98**, 181.
13 J. N. Kondo, M. Uchida, K. Nakajima, D. Lu, M. Hara and K. Domen, *Chem. Mater.*, 2004, **16**, 4304.
14 J. N. Kondo, Y. Takahara, B. Lee, D. Lu and K. Domen, *Top. Catal.*, 2002, **19**, 171.
15 J. N. Kondo, T. Yamashita, K. Nakajima, D. Lu, M. Hara and K. Domen, *J. Mater. Chem.*, 2005, **15**, 2035.
16 D. Li, H. Zhou and I. Honma, *Nat. Mater.*, 2004, **3**, 65.
17 S. Jun, S. H. Joo, R. Ryoo, M. Kruk, M. Jaroniec, Z. Liu, T. Ohsuna and O. Terasaki, *J. Am. Chem. Soc.*, 2000, **122**, 10712.
18 T. Katou, B. Lee, D. Lu, J. N. Kondo, M. Hara and K. Domen, *Angew. Chem., Int. Ed.*, 2003, **42**, 2382.
19 K. Nakajima, M. Hara, K. Domen and J. N. Kondo, *Chem. Lett.*, 2005, **34**, 394.
20 B. Lee, T. Yamashita, D. Lu, J. N. Kondo and K. Domen, *Chem. Mater.*, 2002, **14**, 867.